arXiv:1508.03451v1 [cond-mat.str-el] 14 Aug 2015

Emergent spin-1 trimerized valence bond crystal in the spin-1/2 Heisenberg model on the star lattice

Shi-Ju Ran,[1,2] Wei Li,[3,4] Shou-Shu Gong,[5,6] Andreas Weichselbaum,[3] Jan von Delft,[3] and Gang Su[1,*]

[1]*Theoretical Condensed Matter Physics and Computational Materials Physics Laboratory,*
School of Physics, University of Chinese Academy of Sciences, P. O. Box 4588, Beijing 100049, China
[2]*ICFO-Institut de Ciencies Fotoniques, Avenida Carl Friedrich Gauss, 3, 08860 Castelldefels, Barcelona, Spain*
[3]*Physics Department, Arnold Sommerfeld Center for Theoretical Physics,*
and Center for NanoScience, Ludwig-Maximilians-Universit, Munich 80333, Germany
[4]*Department of Physics, Beihang University, Beijing 100191, China*
[5]*Department of Physics and Astronomy, California State University, Northridge, California 91330, USA*
[6]*National High Magnetic Field Laboratory, Florida State University, Tallahassee, Florida 32310, USA*

We explore the frustrated spin-$1/2$ Heisenberg model on the star lattice with antiferromagnetic (AF) couplings inside each triangle and ferromagnetic (FM) inter-triangle couplings ($J_e < 0$), and calculate its magnetic and thermodynamic properties. We show that the FM couplings do not sabotage the magnetic disordering of the ground state due to the frustration from the AF interactions inside each triangle, but trigger a fully gapped inversion-symmetry-breaking trimerized valence bond crystal (TVBC) with emergent spin-1 degrees of freedom. We discover that with strengthening J_e, the system scales exponentially, either with or without a magnetic field h: the order parameter, the five critical fields that separate the J_e-h ground-state phase diagram into six phases, and the excitation gap obtained by low-temperature specific heat, all depend exponentially on J_e. We calculate the temperature dependence of the specific heat, which can be directly compared with future experiments.

PACS numbers: 75.10.Jm, 75.10.Kt, 75.60.Ej, 05.70.Ln

Introduction.— Two-dimensional (2D) spin-1/2 frustrated magnetic systems [1] are currently of great interest, because they may realize exotic quantum states that do not possess any semi-classical spin ordering [2], such as quantum spin liquids (QSLs) or valence bond crystals (VBCs). Leading candidates for realizing such states are spin-$\frac{1}{2}$ Heisenberg models with competing interactions on, e.g. square, honeycomb and kagomé lattices [3–17]. A particularly promising QSL system that has been argued to have experimental realizations is the kagomé Heisenberg antiferromagnet (KHAF) [18–24]. However the nature of its ground state, i.e., a gapped Z_2 spin liquid [3–6] versus a gapless U(1) Dirac spin liquid [7–10], is still under debate.

Another frustrated 2D quantum system of great potential interest is the Heisenberg model on a star lattice (Fig. 1). Its physics is arguably even richer than that of the KHAF, for several reasons: (a) similar to the kagome lattice, the star lattice bears a high geometrical frustration due to its triangle structure; (b) the star lattice possesses a lower coordination number than the kagome lattice, implying stronger fluctuations; (c) the star lattice naturally involves two inequivalent bonds, which can lead to exotic quantum phases; (d) various QSLs, such as the non-Abelian chiral spin liquid and the double semion spin liquid, have been found in several models on a star lattice, e.g., the Kitaev model and the quantum dimer model [25, 26]; (e) a number of organic iron acetates have been synthesized in experiments [27], which can be described by the Heisenberg model on a star lattice.

However, the properties of the Heisenberg model on a star lattice have not been fully explored yet. Recent research using the large-N approximation and a Gutzwiller projected wavefunction [28] only investigated the system for antiferromagnetic (AF) inter-triangle couplings ($J_e > 0$), where a J_e-dimer VBC and a $\sqrt{3}\times\sqrt{3}$ VBC phase [29] are found (Fig. 1). However, the properties of the system for the ferromagnetic (FM) $J_e < 0$ are still unclear, where the system can be closely related to spin-1 kagomé physics [30–32].

The intrinsic importance of 2D frustrated many-body systems is matched by the great technical challenges involved in studying them. One such challenge is calculating thermodynamic properties, such as specific heat and susceptibility, which can be detected directly in experiments. Most existing studies have, however, focused on the ground-state. Indeed, numerical studies of frustrated quantum magnetic systems at finite temperature are very scarce, owing to the extreme difficulties of such calculations [33–35].

In this Letter, we employ four different state-of-the-art algorithms [34, 36–41] to perform a comprehensive study of the spin-$\frac{1}{2}$ Heisenberg antiferromagnet on the star lattice with FM inter-triangle couplings ($J_e < 0$), calculating its ground state and thermodynamic properties. We show that the FM inter-triangle couplings do not sabotage the magnetic disordering of the ground state that arises due to frustration generated by AF intra-triangle couplings, but, remarkably, trigger a trimerized valence bond crystal (TVBC) with emergent spin-1 degrees of freedom, that breaks spatial inversion symmetry. We determine the phase diagram of the system in a magnetic field and identify six phases. We uncover a magnetization cusp on the boundary between the inversion-symmetry-breaking and the non-inversion-symmetry-breaking phases. We calculate the temperature dependence of the specific heat and determine a non-magnetic gap by analyzing accurate results for the low-temperature behavior of the specific heat. We find that the observables of the system scale exponentially with increasing $|J_e|$, evidenced by the large-J_e dependence of a range of physical quantities, such as the TVBC “order parameter”, five

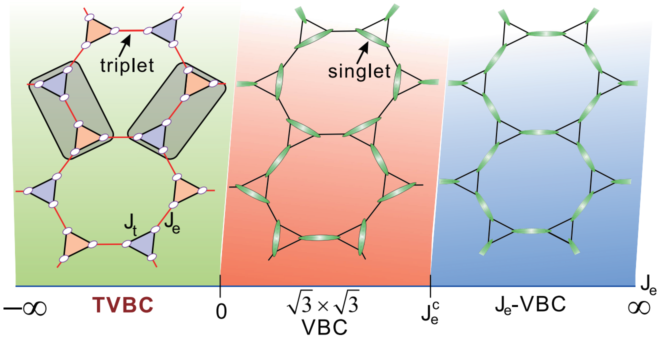

Figure 1: (Color online) The ground-state phase diagram of the star Heisenberg model. For $J_e > 0$, previous studies show various possible VBCs and spin liquids, where one recent work found a $\sqrt{3}\times\sqrt{3}$ VBC and a J_e-bond VBC [28, 29]. The phase boundary J_e^c has not been settled yet. For $J_e < 0$, we show that the system is in a trimerized valence bond crystal (TVBC) phase, where a triplet appears at each J_e bond and the inversion symmetry of up and down triangles (marked by blue and yellow, respectively) is broken.

critical fields and the non-magnetic gap.

Model and methods.— The Hamiltonian of the star Heisenberg model reads

$$H = J_e \sum_{\langle ij\rangle \in J_e} S_i \cdot S_j + J_t \sum_{\langle lm\rangle \in J_t} S_l \cdot S_m, \tag{1}$$

where the first summation runs over all inter-triangle bonds and the second over all intra-triangle bonds. We employ tensor network [37] and DMRG [39] methods to simulate the model on the infinite lattice and cylindrical geometries, respectively. To be specific, the TN representation of the ground state [inset of fig. 2(a)] can be written as

$$|\psi\rangle = \sum_{\{s\}} \mathrm{Tr}_{\{a\}\in \mathrm{TN}}[\prod_j (T(j)^{s_{j,1}s_{j,2}s_{j,3}}_{a_{j,1}a_{j,2}a_{j,3}} |s_{j,1}, s_{j,2}, s_{j,3}\rangle)], \tag{2}$$

where $T(j)$ is a ($d^3 \times D^3$) tensor residing on the j-th triangle with physical dimension d and ancillary bond dimension D, containing all parameters of the TN state. The ancillary bonds $\{a_{j,n}\}$ ($n = 1, 2, 3$) carry the entanglement of the state and $\mathrm{Tr}_{\{a\}\in\mathrm{TN}}$ denotes a contraction of all shared $\{a_{j,n}\}$. The physical bonds $\{s_{j,n}\}$ ($n = 1, 2, 3$) represent the three spins inside the j-th triangle with local basis $|s_{j,n}\rangle$. Such a TN ansatz is called a projected entangled-pair state (PEPS) [40]. The simple update algorithm provides an efficient way to optimize the PEPS by minimizing the energy per site $E_0 = \langle\psi|H|\psi\rangle$.

In addition, we implement SU(2) symmetry in TN states and related algorithms by using QSpace techniques [41]: we impose SU(2) symmetry in every single tensor index, retain the symmetry during imaginary time evolutions and other tensor manipulations, keep track of multiplets (instead of individual states) on the bonds, and manipulate only reduced tensors (instead of full tensors), thus reducing both the memory and CPU time dramatically [30, 41].

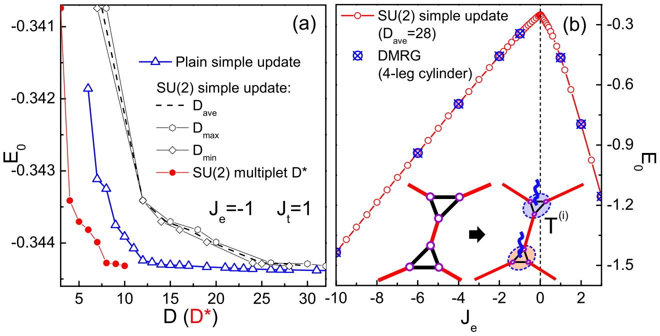

Figure 2: (Color online) (a) The ground-state energy E_0 of the star Heisenberg model for $J_e = -1$ and $J_t = 1$ obtained by the plain and SU(2) simple update algorithm, where E_0 converges versus number of states (D) and number of multiplets (D^* red solid dots), respectively, with clearly superior performance of the SU(2)-based calculations. For comparison only, we also translate the number of multiplets D^* into the corresponding actual number of states D (black lines and symbols). Since for fixed D^*, D may vary (depending on the specific set of multiplets associated with each virtual bond), we show the minimum, maximum and average value of D over the three virtual bond indices of a tensor. (b) E_0 versus J_e, obtained by SU(2) simple update and DMRG simulations, which show very good agreement with each other in the whole parameter range. The inset sketches the local tensors of the TN state.

First, we compare the ground-state energy obtained by different methods. In Fig. 2(a), we show the energy obtained by plain and SU(2) PEPS calculations, which both converge to the same results. Note that for comparable number of states D, a lower ground state energy can be obtained by plain PEPS as compared to SU(2) PEPS, since it is allowed to break symmetries and hence has access to a larger variational parameter space. However, the results converge towards the same value for large D, suggeting that as expected, the tensors eventually converge to tensors that respect symmetries. This justifies the exploitation of symmetries at significantly reduced overall numerical cost.

In Fig. 2(b) we show the energy obtained from SU(2) TN simulations and cylindrical DMRG for $-10.0 \leq J_e \leq 3.0$, which show an excellent agreement in the whole region. Moreover, the appearance of a cusp in the energy curve at $J_e = 0$ indicates a first-order phase transition.

Spontaneous inversion symmetry breaking.— We now study the ground state of the star model, which is found to possess spontaneous inversion symmetry breaking (SISB). It can be characterized by the energy difference between the two kinds of triangles $\delta \equiv |E^{\Delta} - E^{\nabla}|$ where we have $E^{\Delta(\nabla)} = \langle\psi| \sum_{\langle ij\rangle\in\Delta(\nabla)} H_{ij} |\psi\rangle$ per triangle with the summation running over all local interactions H_{ij} inside the up (down) triangles. We use DMRG to calculate the cylinder system with the geometry shown in Fig. 3(a) (denoted by YC4). To break the inversion symmetry between the up and down triangles, we take the couplings inside the up triangles on the open boundaries as $J_{\mathrm{pin}} = 2J_t$ (J_t is the coupling constant for all other triangles). Then, we can measure the decaying behavior

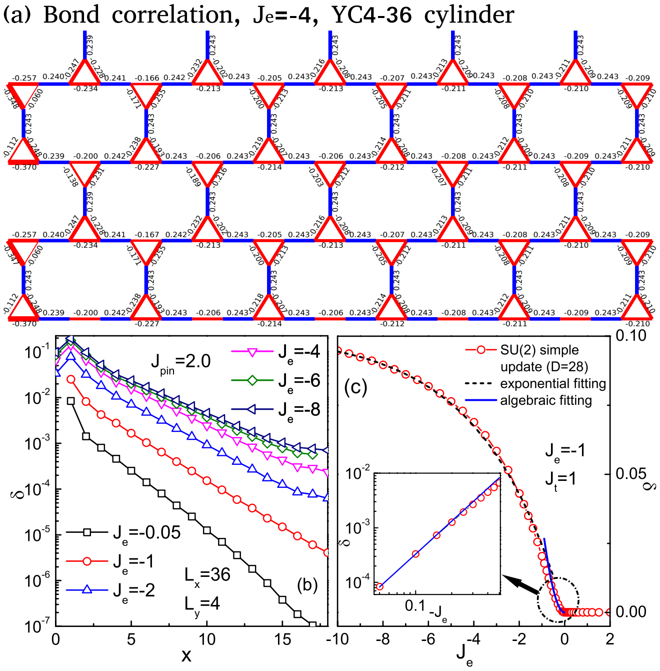

Figure 3: (Color online) (a) The bond correlation $\langle S_i \cdot S_j \rangle$ versus distance x from the pinned boundary (using $J_{\rm pin} = 2$) on a YC4-36 cylinder for $J_e = -4$ calculated by DMRG keeping 2000 SU(2) multiplets. (b) Log-linear plot of the inversion symmetry breaking parameter δ as function of the distance x from the boundary for the YC4-36 cylinder with boundary pinning. (c) The J_e dependence of δ obtained from SU(2) simple update simulations. As long as $J_e < 0$, the system has a non-zero δ. We find by fitting that for approximately $-J_e \gg 4$, δ fulfills the relation $\delta = \tilde{\delta}(1 - e^{\mu J_e})$, where $\mu = 0.28$ and $\tilde{\delta} = 0.1$ that gives the value of δ for $J_e \to -\infty$. In contrast, for small $|J_e|$ we find that δ satisfies $\delta = 0.03 J_e^2$ for $J_e \to 0$ (see inset).

of δ from the boundary to the bulk. As shown in Fig. 3(b), we find that δ decays quite slowly, implying a large decay length for large $|J_e|$. We checked that different values of $J_{\rm pin}$ give the same decay length. Since a non-symmetry-breaking state just possesses a short decay length, our calculations strongly suggest a ground state with SISB on a wider system. With decreasing $|J_e|$, δ decays faster. For small values of $|J_e|$, the SISB is too weak to identify on a small cylinder. Thus, we employ the TN simulations on the infinite-length system.

The order parameter δ obtained from TN methods is shown in Fig. 3(c). For large $|J_e|$, TN calculations, too, find a strong TVBC order, consistent with DMRG results. By fitting δ with $-J_e \gg 0$, we find that δ fulfills an exponential behavior with J_e as

$$\delta = \tilde{\delta}(1 - e^{\mu J_e}), \tag{3}$$

where we have $\mu = 0.28$ and $\tilde{\delta} = 0.1$. It indicates that the large $|J_e|$ couplings project each corresponding spin-$\frac{1}{2}$ pair into an effective $S = 1$ spin, and stabilize a TVBC. Interestingly, for the small $|J_e|$ region, the TN simulations show that the inversion symmetry is broken for any small $J_e < 0$, while such a symmetry is found to be intact for $J_e > 0$. To be specific, for $-J_e \to 0$, δ satisfies the algebraic relation $\delta = 0.03 J_e^2$, as shown in the inset of Fig. 3 (c). Our results not only support the TVBC ground state for the spin-1 kagomé model [30–32], but also further show that such a TVBC is robust in the spin-$\frac{1}{2}$ star model for any finite FM J_e interaction, where each two spin-$\frac{1}{2}$ connected by J_e cannot be regarded as strictly projected into an effective spin-1.

Ground-state phase diagram in magnetic fields.— In a magnetic field, frustrated magnetic systems usually exhibit singularities in the magnetization curve such as cusps [42] and plateaus [43], which reveal the exotic structure of the energy spectrum and distinguish different phases. We study the field dependence of the magnetization per site M_z and the energy difference δ, as shown in Fig. 4. Interestingly, we find a zero plateau corresponding to a finite spin gap, a cusp representing the restoration of inversion symmetry, and a $1/3$-plateau in the magnetization curve.

In the zero plateau region, $h < h_{c1}$, both M_z and δ remain unchanged, indicating that there is a finite spin gap protecting the TVBC state. With increasing h, the spin gap decreases and eventually closes at $h = h_{c1}$. For $h > h_{c1}$, M_z becomes nonzero and δ starts to decrease. At $h = h_{c2}$, a cusp appears in M_z and δ vanishes, separating the SISB phase from non-SISB phases. A magnetization cusp has also been observed in some one-dimensional frustrated magnetic systems having ground states that break lattice symmetry, reflecting the novel energy dispersion of the low-lying excitations [42]. A first shoulder in the magnetization occurs consistently around $M \simeq 1/30$. By further increasing the field, we find a $1/3$-plateau corresponding to a gapped solid state [43]. Based on the behaviors of M_z and δ we obtain the quantum phase diagram in the J_e-h plane, shown in Fig. 4(c).

We find that the critical fields h_{ci} ($i = 1, 2, \cdots, 5$) also converge exponentially for large $|J_e|$,

$$h_{ci} = \tilde{h}_{ci}(1 - \alpha_i e^{\nu_i J_e}), \tag{4}$$

as shown in Fig. 4(c), with coefficients given in Table I. The scaling behavior of the critical fields strongly implies that the star Heisenberg model approaches the effective spin-1 model in an exponential manner, suggesting that the large $|J_e|$ represents a gapped system, consistent with [30–32].

Specific heat.—To study the thermodynamics and the low-lying excitations, we calculate the temperature dependence of the specific heat, employing the network contractor dynamics (NCD) method [34] that is based on a TN representation of the finite-temperature density matrix. In experiments, the specific heat can be measured by mature techniques, e.g. a thermal relaxation calorimeter.

As shown in Fig. 5(a), by taking J_e from zero to $-\infty$, the low-temperature peak moves to higher temperature and merges with other peaks. From the inset of Fig. 5(a), one can see that below the low-temperature peak, $\ln C$ depends linearly on the inverse temperature $1/T$ as $\ln C = -\Delta/T + {\rm const.}$, indicating a finite gap Δ that is consistent with the gapped TVBC ground state. The J_e-dependence of Δ is given

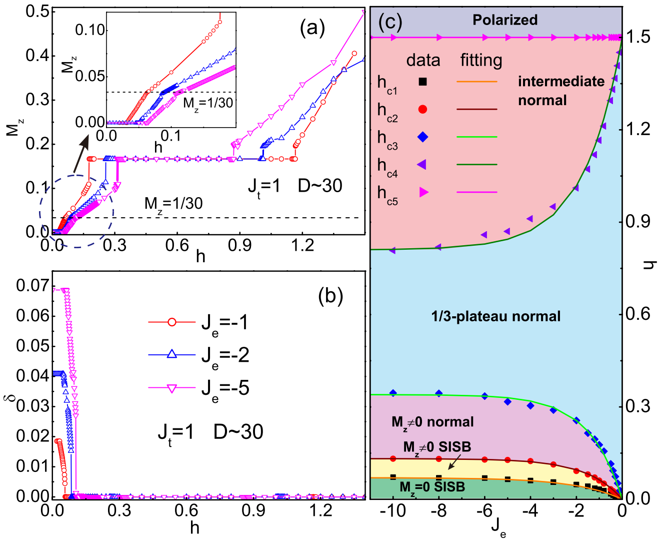

Figure 4: (Color online) The field-dependence of (a) the magnetization M_z and (b) the TVBC order parameter δ. Five critical fields h_{ci} ($i = 1, 2, \cdots, 5$) is determined by M_z and δ, which determine six phases in the J_e-h diagram as shown in (c). For $0 \leq h < h_{c1}$, $M_z = 0$ and δ is intact. For $h_{c1} < h < h_{c2}$, M_z increases, and δ starts to diminish and vanishes at $h = h_{c2}$, where the inversion symmetric and broke phases are separated and one always has $M_z = 1/30$. For $h_{c3} < h < h_{c4}$, the system is in a conventional $1/3$-plateau solid phase.

in Fig. 5(b). We observe that Δ also converges exponentially for large $|J_e|$

$$\Delta = \tilde{\Delta}(1 - e^{\kappa J_e}), \tag{5}$$

where a fit yields $\kappa = 0.5$ and $\tilde{\Delta} = 0.17 \pm 0.02$ corresponding to the gap for $J_e \to -\infty$. We suggest that the Δ obtained via the specific heat is the non-magnetic singlet-singlet (not singlet-triplet) gap, since SU(2) symmetry is preserved at all temperatures, evidenced by the vanishing finite-temperature magnetization. This is consistent with the spin-1 kagomé calculation [44], where a non-magnetic gap $\tilde{\Delta} = 0.1 \sim 0.2$ is obtained.

The non-magnetic gap is larger than the spin gap, implying that there are no singlet states lying under the first triplet excitation, thus the TVBC is fully gapped. This is consistent with the fact that the magnetic field h_{c2}, at which inversion symmetry is recovered, is larger than h_{c1}, at which the spin gap closes.

Table I: Values for the fitting parameters $\tilde{h}_{ci}$, α_i and ν_i of the critical fields [see Eq. (4)]. Note that as $h_{c5} = 1.5$ is a constant, we have $\alpha_5 = 0$ and any ν_5.

	h_{c1}	h_{c2}	h_{c3}	h_{c4}	h_{c5}
$\tilde{h}_{ci}$	0.07	0.132	0.34	0.81	1.5
α_i	1	1	1	-0.85	0
ν_i	0.5	0.65	0.7	0.6	$*$

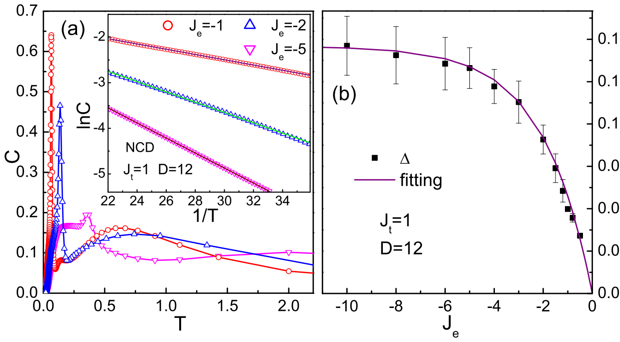

Figure 5: (Color online) (a) The temperature-dependence of specific heat C for various J_e, where multi-peak structures are observed. The position of the low-temperature peak moves to the higher temperature as $-J_e$ increases. Inset: the curve of $\ln C$ versus inverse temperature $1/T$. Below the low-temperature peak, one can see that the specific heat decays exponentially with $1/T$ as $\ln C = -\Delta/T + \text{const}$, where Δ is the (J_e-dependent) excitation gap. (b) By fitting specific heat, the excitation gap Δ for different J_e is obtained and shown to fulfill the relation $\Delta = \tilde{\Delta}(1 - e^{\kappa J_e})$. The error bars are given by the linearity of the low temperature C. By fitting the $\Delta - J_e$ curve, we have $\tilde{\Delta} = 0.175$ that gives the excitation gap in the $J_e \to -\infty$ limit and the constant $\kappa = 0.5$.

Conclusions.— We discover an emergent spin-1 TVBC with spontaneous lattice-inversion-symmetry breaking in the spin-$\frac{1}{2}$ star Heisenberg model with FM inter-triangle coupling J_e, and study its ground-state and thermodynamic properties. The reliability is confirmed by four different algorithms including SU(2) DMRG, simple update of the TN state with and without SU(2) symmetry, and NCD. Our results not only support the conclusion of a TVBC state in the ground state of the spin-1 kagomé Heisenberg model [30–32, 44], but also reveal the rich properties of the spin-$\frac{1}{2}$ star system, including fruitful phases in a magnetic field, magnetic cusps at $M_z \simeq 1/30$ and exponential scaling behavior for $J_e \to -\infty$. Our work implies that spin-1 VBCs may emerge in the geometrically frustrated spin-$\frac{1}{2}$ systems with FM interactions. Moreover, our calculations of the specific heat present an efficient way to obtain the excitation gap of 2D frustrated many-body systems. It also provides valuable information at finite temperatures which can be compared directly with future experiments.

Acknowledgements.— We are indebted to C. Peng for useful discussions. This work was supported in part by the MOST of China (Grants No. 2012CB932900 and No. 2013CB933401), the Strategic Priority Research Program of the Chinese Academy of Sciences (Grant No. XDB07010100), and NSFC Grant No. 11474249. S.S.G. is supported by the National Science Foundation through grant DMR-1408560, and the National High Magnetic Field Laboratory that is supported by NSF DMR-1157490 and the State of Florida. W.L. was supported by SFB-TR12, A.W. by DFG WE4819/1-1 and WE4819/1-2. S.J.R. is supported by ERC ADG OSYRIS and Spanish Ministry grant FOQUS, and would like to thank Maciej Lewenstein for partly supporting a visit to LMU through

ERC ADG OSYRIS.

---

[*] Corresponding author. Email: gsu@ucas.ac.cn

[1] L. Balents, Nature **464**, 199 (2010).

[2] H. T. Diep, *Frustrated spin systems*. World Scientific, 2004.

[3] S. Yan, D. Huse, and S. R. White, Science **332**, 1173-1176 (2011).

[4] S. Depenbrock, I. P. McCulloch, and U. Schollwöck, Phys. Rev. Lett. **109**, 067201 (2012).

[5] H. C. Jiang, Z. H. Wang and L. Balents, Nat. Phys. **8**, 902-905 (2012).

[6] S. Nishimoto, N. Shibata and C. Hotta, Nat. Commun. **4**, 2287 (2013).

[7] Y. Ran, M. Hermele, P. A. Lee, and X. G. Wen, Phys. Rev. Lett. **98**, 117205 (2007).

[8] M. Hermele, Y. Ran, P. A. Lee, and X.-G. Wen, Phys. Rev. B **77**, 224413 (2008).

[9] Y. Iqbal, F. Becca, S. Sorella, and D. Poilblanc, Phys. Rev. B **87**, 060405(R) (2013).

[10] Y. Iqbal, D. Poilblanc, and F. Becca, Phys. Rev. B **89**, 020407(R) (2014).

[11] Y. C. He, D. N. Sheng, and Y. Chen, Phys. Rev. Lett. **112**, 137202 (2014).

[12] S. S. Gong, W. Zhu, and D. N. Sheng, Sci. Rep. **4**, 6317 (2014).

[13] B. Bauer, L. Cincio, B. P. Keller, M. Dolfi, G. Vidal, S. Trebst, and A. W. W. Ludwig, Nat. Commu. **5**, 5137 (2014).

[14] R. Ganesh, Jeroen van den Brink, and S. Nishimoto, Phys. Rev. Lett. **110**, 127203 (2013).

[15] Z. Y. Zhu, D. A. Huse, and S. R. White, Phys. Rev. Lett. **110**, 127205 (2013).

[16] S. S. Gong, D. N. Sheng, O. I. Motrunich, and M. P. A. Fisher, Phys. Rev. B **88**, 165138 (2013).

[17] S. S. Gong, W. Zhu, D. N. Sheng, O. I. Motrunich, and M. P. A. Fisher, Phys. Rev. Lett. **113**, 027201 (2014).

[18] P. Mendels, F. Bert, M. A. de Vries, A. Olariu, A. Harrison, F. Duc, J. C. Trombe, J. S. Lord, A. Amato, and C. Baines, Phys. Rev. Lett. **98**, 077204 (2007).

[19] J. S. Helton, K. Matan, M. P. Shores, E. A. Nytko, B. M. Bartlett, Y. Yoshida, Y. Takano, A. Suslov, Y. Qiu, J.-H. Chung, D. G. Nocera, and Y. S. Lee, Phys. Rev. Lett. **98**, 107204 (2007).

[20] M. A. de Vries, J. R. Stewart, P. P. Deen, J. O. Piatek, G. J. Nilsen, H. M. Rnnow, and A. Harrison, Phys. Rev. Lett. **103**, 237201 (2009).

[21] D. Wulferding, P. Lemmens, P. Scheib, J. Röder, P. Mendels, S. Chu, T. Han, and Y. S. Lee, Phys. Rev. B **82**, 144412 (2010).

[22] B. Fåk, E. Kermarrec, L. Messio, B. Bernu, C. Lhuillier, F. Bert, P. Mendels, B. Koteswararao, F. Bouquet, J. Ollivier, A. D. Hillier, A. Amato, R. H. Colman, and A. S. Wills, Phys. Rev. Lett. **109**, 037208 (2012).

[23] T. H. Han, J. S. Helton, S. Chu, D. G. Nocera, J. A. Rodriguez-Rivera, C. Broholm, and Y. S. Lee, Nature **492**, 7429 (2012).

[24] L. Clark, J. C. Orain, F. Bert, M. A. De Vries, F. H. Aidoudi, R. E. Morris, P. Lightfoot, J. S. Lord, M. T. F. Telling, P. Bonville, J. P. Attfield, P. Mendels, and A. Harrison, Phys. Rev. Lett. **110**, 207208 (2013).

[25] H. Yao and S. A. Kivelson, Phys. Rev. Lett. **108**, 247206 (2012).

[26] Y. Qi, Z. C. Gu, and H. Yao, Arxiv:1406.6364.

[27] Y. Z. Zheng, M. L. Tong, W. Xue, W. X. Zhang, X. M. Chen, F. Grandjean, and G. J. Long, Angew. Chem. Int. Ed. **46**, 6076 (2007).

[28] B. J. Yang, A. Paramekanti, and Y. B. Kim, Phys. Rev. B **81**, 134418 (2010).

[29] Note that some former researches by the eaxct diagonalization, large-N Sp(N) mean field theory and projective symmetry group analysis also indicated other possible VBCs and QSLs. See e.g. J. Richter, J. Schulenburg, A. Honecker, and D. Schmalfuß Phys. Rev. B **70**, 174454 (2004); G. Misguich and P. Sindzingre, J. Phys.: Condens. Matter **19**, 145202 (2007); T. P. Choy and Y. B. Kim, Phys. Rev. B **80**, 064404 (2009).

[30] T. Liu, W. Li, A. Weichselbaum, J. von Delft, G. Su, Phys. Rev. B **91**, 060403(R) (2015).

[31] H. J. Changlani and A. M. Läuchli, Phys. Rev. B **91**, 100407(R) (2015).

[32] T. Picot and D. Poilblanc, Phys. Rev. B **91**, 064415 (2015).

[33] S. J. Ran, W. Li, B. Xi, Z. Zhang, and G. Su, Phys. Rev. B **86**, 134429 (2012).

[34] S. J. Ran, B. Xi, T. Liu, and G. Su, Phys. Rev. B **88**, 064407 (2013).

[35] P. Czarnik, L. Cincio, and J. Dziarmaga, Phys. Rev. B **86**, 245101 (2012); P. Czarnik and J. Dziarmaga, Phys. Rev. B **90**, 035144 (2014); **92**, 035120 (2015).

[36] M. Levin and C. P. Nave, Phys. Rev. Lett. **99**, 120601 (2007).

[37] H. C. Jiang, Z. Y. Weng, and T. Xiang, Phys. Rev. Lett. **101**, 090603 (2008); Z. Y. Xie, H. C. Jiang, Q. N. Chen, Z. Y. Weng, and T. Xiang, *ibid* **103**, 160601 (2009).

[38] Z. C. Gu, M. Levin, and X. G. Wen, Phys. Rev. B **78**, 205116 (2008); Z.C. Gu and X. G. Wen, Phys. Rev. B **80**, 155131 (2009).

[39] S. R. White, Phys. Rev. Lett. **69**, 2863 (1992), Phys. Rev. B. **48**, 10345 (1993).

[40] F. Verstraete and J. I. Cirac, arXiv:cond-mat/0407066; J. Jordan, R. Orús, G. Vidal, F. Verstraete, and J. I. Cirac, Phys. Rev. Lett. **101**, 250602 (2008).

[41] A. Weichselbaum, Anna. of Phys. **327**, 2972-3047 (2012).

[42] K. Okunishi, Y. Hieida, and Y. Akutsu, Phys. Rev. B **60**, R6953(R) (1999).

[43] M. Oshikawa, M. Yamanaka, and I. Affleck, Phys. Rev. Lett. **78**, 1984 (1997).

[44] Private communications with H. J. Changlani and A. M. Läuchli.